

Water adsorption and dissociation on gold catalysts supported on anatase-TiO₂(101)

H. Valdés, L. M. Molina, J. A. Alonso

Departamento de Física Teórica, Atómica y Óptica, Universidad de Valladolid, E-47011 Valladolid, Spain.

Abstract

The presence of water can strongly affect the reactivity of gold catalysts. For this reason, ab initio density functional simulations have been performed to study the adsorption and dissociation of water on the anatase-TiO₂(101) surface, both clean and in the presence of a supported model gold nanocluster, Au₄. When adsorbed not too close to the cluster, water is adsorbed and dissociated with roughly the same binding energies and dissociation barriers as in the catalyst-free surface. If the molecule adsorbs at the Au/TiO₂ perimeter interface, making contact with gold, we find a slight stabilization of molecular water, whereas dissociated water becomes slightly less stable. The preferential mechanism for water dissociation is found to be a splitting of the H-OH bond at the TiO₂ surface, with the gold cluster playing a minor role. Calculations of the relative stability of various water-related species show that the gold catalyst favours accumulation of excess hydroxyls around its perimeter.

Keywords: DFT calculations; gold catalysts; TiO₂; water; reaction intermediates

1. Introduction

Titanium dioxide is one of the best studied metal oxides due to its wide range of technological applications in catalysis, photochemistry and electrochemistry [1, 2]. In particular, it is one of the most commonly used oxide supports for model nanocatalysts. In the last ten years, it has been routinely employed as a support for gold nanoparticles, which show very promising catalytic activity for various chemical reactions, like CO oxidation, water gas shift, propene epoxidation, etc. [3–5].

It has been reported that the presence of water, even at small concentrations, can strongly affect the reactivity of the gold catalysts [6, 7] for a wide range of chemical reactions. Water can influence a given reaction in various ways, the most obvious one by interacting with the reactants or with the products directly at the gold catalyst. Also, the surface hydroxylation can strongly affect

the global reactivity, since the Au/TiO₂ perimeter interface acts frequently as a favorable reaction region [8, 9]. The presence in such region of either intact or dissociated water is expected to affect the binding of either reactants or intermediate compounds, thus altering the reaction mechanisms [10, 11]. The interaction of gold clusters and nanoparticles with the TiO₂ surface is likely to cause electrons to be transferred between the metal cluster and the surface [12–14], thus changing the stability of neighbouring adsorbed water or hydroxyl groups.

Among the various titania forms that have been employed as supports, one of the most interesting is anatase [15]. It is now established that, under standard reaction conditions (where a sizable partial pressure of water vapor can be present) clean anatase will adsorb and dissociate water, partially saturating the surface dangling bonds with hydroxyl groups [16–18]. However, little is known about the effects that supported catalysts can cause on the ability of the TiO₂ substrate to bind and dissociate H₂O [19, 20]. The metal-oxide interaction may cause substantial changes on the way water interacts with the oxide at the cluster-oxide perimeter interface, altering the preferred equilibrium coverages, the ratio of dissociated vs molecular water, or even the relative concentration of OH and H groups. Also, the presence of the metal could induce a preferential adsorption of water into it, and could also offer low energy barriers for water dissociation at its surface, with perhaps an important spill-over effect.

This has motivated us to perform a complete study of the way water interacts with titania-supported gold catalysts. Using the Density Functional Theory (DFT) we have analyzed the energetics of both molecular and dissociated water adsorption at the Au/TiO₂ perimeter interface. Besides simulating water adsorption at various coverages, we have also studied in detail the reaction pathways for water dissociation on these model catalysts, and the associated activation barriers. Finally, we have also explored the possibility of an unbalance in the relative OH and H concentrations caused by the presence of the gold catalyst.

2. Computational setup

Density Functional Theory (DFT) calculations were carried out using the GPAW code [21, 22]. The Perdew-Burke-Ernzerhof (PBE) [23, 24] Generalized Gradient Approximation (GGA) for the exchange-correlation functional was used throughout this work. The following orbitals were considered as valence: 1s for hydrogen, 2s and 2p orbitals for oxygen, and 3s, 3p, 3d and 4s orbitals for titanium (in this latter case, inclusion of 3s and 3p electrons as valence is convenient in order to avoid errors due to core-polarization). For each geometry, wave functions are optimized until the total energy changes less than 0.0001 eV between iterations, and the electronic density less than 0.0003 e⁻/Å³. Spin polarized calculations were carried out for open-shell species. The (101) surface of TiO₂ anatase was represented by a slab formed by two O-Ti-O trilayers, the first one allowed to relax while all the atoms of the bottom layer were fixed at their bulk positions.

For the simulations of the bare anatase (101) surface (that is, without a supported gold catalyst), we have chosen a 1×3 periodic unit cell, with lateral dimensions of $10.8 \text{ \AA} \times 11.4 \text{ \AA}$. This size is large enough to prevent sizable interactions between adsorbed species in neighbour cells. Also, it allows us to study the variation of binding energies with increasing coverage, of up to six water molecules. As a model of a supported gold nanocatalyst, we have placed a Au_4 cluster on top of the TiO_2 -anatase surface. We choose such small size in order to keep the simulation cell as small as possible. Besides, many experimental studies have shown that small clusters with various sizes can be easily deposited on the TiO_2 surface, being highly active catalysts for a broad class of reactions [25–27]. For supported Au_4 , we use a 1×4 anatase unit cell. The larger lateral dimensions are needed both for keeping Au_4 clusters in neighbour cells far from each other, as well as for having enough available surface sites around the gold cluster to study water adsorption. In both cases, we have a vacuum space of 10 \AA in the vertical direction, which provides enough separation between the adsorbed species and the edge of the unit cell. A broad variety of conformations for the supported cluster were tested; among several conformers with almost equal binding energies, we have chosen a rhombus structure which is adsorbed obliquely to the surface (see Figure 6). In all cases, for economy purposes, we have used a single k point. The large unit cell size makes the use of a $(1 \times 1 \times 1)$ Monkhorst-Pack sampling a reasonable approximation. In our tests, larger $(2 \times 2 \times 1)$ or $(3 \times 3 \times 1)$ samplings modify the H_2O binding energy only by a mere 0.001 eV . For some selected cases, Van der Waals dispersion contributions to the water binding energies were calculated perturbatively using Grimme’s DFT-D3 semiempirical approximation [28]. Since we are studying a perfect TiO_2 surface with no defects, we do not expect a substantial amount of self-interaction (which, of course, is much larger for systems including oxygen vacancies). This has motivated us to use a pure DFT approach, instead of reporting semiempirically corrected DFT+U energies. While inclusion of this correction can help on improving the description of the electronic structure (band gap size, for example), it is not clear that it will result on sizable changes for the calculated water adsorption energies. Recently, Kumar et al. have analyzed the effect of both DFT+U and VdW semiempirical corrections on the binding energy of water on rutile TiO_2 [29], finding that +U corrections to water binding energy are very small (not larger than 0.05 eV), actually smaller than VdW corrections. In the cases of clean anatase- TiO_2 and Au_4 supported on it, we expect a similar behaviour, with pure DFT binding energies being reasonable enough.

Geometries were fully relaxed using the BFGS algorithm [30] until the maximum force was converged with a precision of 0.02 eV/\AA^{-1} . This criteria results in total energies for the relaxed structures with a precision of the order of 0.001 eV . Energy barriers for water dissociation and hydrogen transfer reactions were calculated by a constrained minimization method, involving several simulations where the reaction coordinate (H-O bond distance) was restricted at monotonously decreasing values, while allowing the rest of the system to freely relax [31]. Transition state structures were characterized as energy maxima in the reaction profile; because of the complexity of the potential energy surface for

the adsorbed molecule, we took care of checking the saddle point character at the transition state by relaxing various candidate conformations at the critical value of the reaction coordinate. With this procedure, we obtained a precision for the calculated barrier heights of the order of 0.01 eV.

3. Water adsorption at the (101) surface of clean anatase TiO₂

Before studying the adsorption of water at the Au₄/TiO₂ system, it is necessary to understand the features of water binding in the absence of the gold catalyst. Then by comparing both results, we can obtain useful information on the effect that the supported catalyst produces on the surface, by checking for any tendency of adsorbed water to concentrate around the catalyst.

Let us start by reporting the results for molecular adsorption of water at the (101) surface of clean anatase. Figure 1 collects the equilibrium structures for adsorption of up to six water molecules at the TiO₂ surface. This covers all the range of water surface coverage, from minimal (16%) up to complete (100%). For the sake of clarity only the upper part of the slab of the 1×3 unit cell of anatase (101) is shown in the Figure. The total binding energies, $E_b(n)$, for these configurations are also included. These are calculated as the energies required to disassemble the system into the separate parts, TiO₂ and n isolated water molecules:

$$E_b(n) = nE(H_2O, gas) + E(TiO_2) - E((nH_2O)/TiO_2), \quad n = 1, \dots, 6 \quad (1)$$

Therefore, positive values of $E_b(n)$ mean that H₂O binding is thermodynamically favourable. In agreement with previous studies, we find an easy chemisorption of water molecules on top of the five-fold coordinated Ti atoms at the surface. From now on, we will label these sites as Ti5c. The bond distances between the oxygen atom of H₂O and the Ti5c range from 2.28 Å ($n = 1$) to 2.36 Å ($n = 6$). $E_b(n)$ increases steadily as the number of adsorbed water molecules increases. Besides the pure DFT results, we have also evaluated the contribution to the adsorption energies due to dispersive VdW interactions. In all the cases, such contribution has a fairly constant value of the order of 0.17 eV per molecule, which represents about 20% of the total binding energy.

In order to check whether the water molecules adsorb independently from each other, or there is any kind of saturation effects, we have calculated the successive binding energies for each new water molecule adsorbed on the TiO₂ surface, $\Delta E_b(n)$:

$$\Delta E_b(n) = E_b(n) - E_b(n - 1), \quad n = 1, \dots, 6 \quad (2)$$

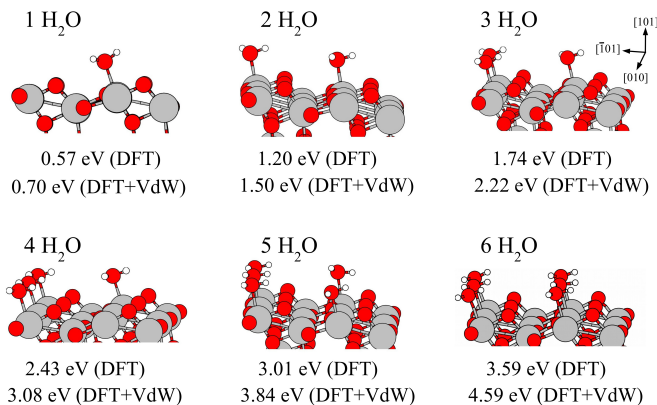


Figure 1: Equilibrium structures and binding energies (E_b ; in eV) of one to six water molecules adsorbed on the anatase-TiO₂(101) surface. In every case, both DFT and DFT-VdW values for E_b (using DFT-D3 semiempirical correction) are given. The titanium atoms are coloured in grey, the oxygen atoms in red and the hydrogen atoms in white.

The results (which compare DFT and DFT+VdW values) are reported in Table 1. They show that in all cases the DFT energy required to adsorb new water molecules departs little from its average value of around 0.6 eV. This confirms that molecular water, at high partial pressures, is expected to cover the surface by saturating most of the surface Ti sites.

n	1	2	3	4	5	6
$\Delta E_b(n)$ (DFT)	0.57	0.63	0.54	0.68	0.59	0.58
E_{VdW}	0.13	0.17	0.18	0.17	0.18	0.17
$\Delta E_b(n)$ (DFT+VdW)	0.70	0.80	0.72	0.85	0.77	0.75

Table 1: Successive binding energies $\Delta E_b(n)$ for the adsorption of water molecules on TiO₂. Energies are given in eV. Both DFT and DFT-VdW data (using DFT-D3 semiempirical correction) are given.

Next, we have calculated the energy barrier for water dissociation at the anatase-TiO₂(101) surface. In order to analyze the influence of coverage effects, we have considered three different situations, with the results being shown in Figure 2. In all cases, we calculate the reaction energy barrier for the dissociation of a water molecule adsorbed at a Ti5c site, by plotting the evolution of the energy of the system along the HO—H—O_{2c} reaction coordinate (namely, the distance between the hydrogen atom of water and the two-fold coordinated O_{2c} surface oxygen atom). The insets show the structures for the initial, transition, and final states. In order to establish a more direct comparison with the similar results for the Au₄/TiO₂ system (to be presented later in the paper), we have performed these calculations in the same anatase (101) (1×4) unit cell.

The top panel shows the results for water adsorbed on a clean anatase-

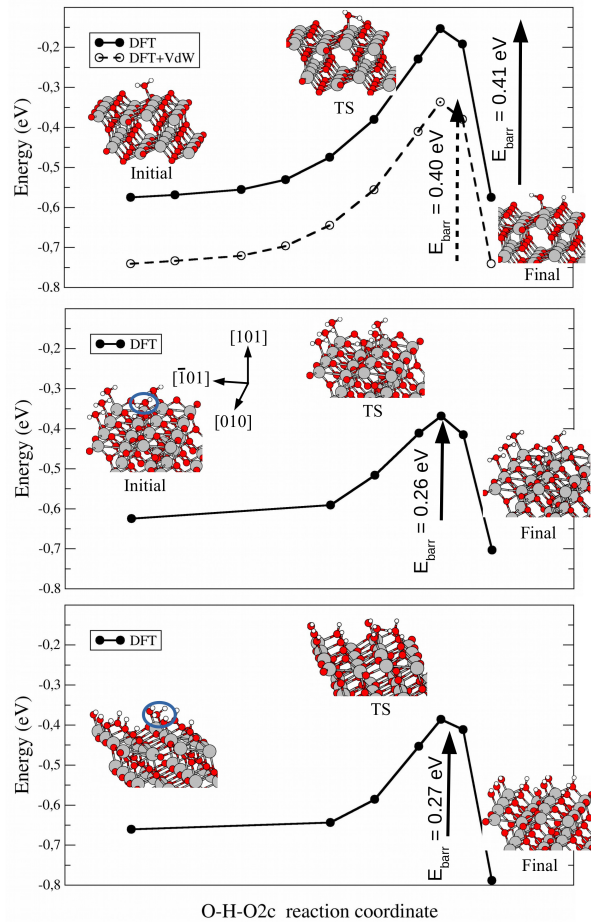


Figure 2: Barriers for dissociation (in eV) of one water molecule on the anatase (101) surface. The top panel shows the results for water adsorbed at a clean TiO_2 surface. The dashed line represents VdW-corrected energies. Insets show the structures of the initial, transition and final states. The middle and lower panels show the dissociation process for the surface precovered with five additional water molecules, either intact or dissociated. The blue circles mark the location of the dissociating H_2O molecule. The zero of energies is taken as the sum of energies of a gas phase H_2O molecule and the TiO_2 anatase surface without it (either clean or with five adsorbed water molecules).

$\text{TiO}_2(101)$ surface. Initially, water adsorbs with a binding energy of 0.57 eV. For this configuration, the distance between the oxygen atom of the water molecule and the Ti5c atom is 2.29 Å, and the $\text{H}-\text{O}2\text{c}$ distance is equal to 2.26 Å. The transition state is found at a moderate barrier height of 0.41 eV; in this state the H atom is located at the middle point between HO and one $\text{O}2\text{c}$ atom,

$d(\text{HO—H}) = d(\text{H—O2c}) = 1.2 \text{ \AA}$, and the length of the HO—Ti5c bond is 2.08 \AA , slightly shorter compared to the initial configuration. Finally, in the dissociated state, the binding energy is $E_b = 0.49 \text{ eV}$, the HO—Ti5c distance is equal to 1.85 \AA , and the H-O2c bond distance is 0.98 \AA . In summary, the results indicate that at relatively low temperatures water easily dissociates at the clean anatase surface (with the final dissociated state being only marginally less stable than the initial molecular state). In the figure, we also compare the pure DFT energies with the VdW-corrected values (dashed curve). The results confirm that including dispersive interactions (with a fairly constant 0.18 eV value) only alters the overall H_2O binding energy, with the barrier energy being almost unchanged. It is worth mentioning that our calculated water binding energies and barrier heights are in good agreement with data from other DFT studies of water interaction with TiO_2 [32–34].

The middle and low panels show the energy barriers for the cases of water dissociating at anatase- $\text{TiO}_2(101)$ surfaces precovered with a high amount of water, either molecularly or dissociatively adsorbed. The main effect caused by the large water coverage is a stabilization of both transition and final states, which lowers the reaction barrier by about 0.15 eV . Such stabilization is due to a tendency of the dissociating water molecule to form weak hydrogen bonds with its neighbour water molecules or hydroxyl groups. Therefore, we can conclude that increasing water coverages favour the process of dissociative adsorption for additional water molecules.

Now, we consider the issue of whether water dissociation at the surface is an extensive phenomenon, not being restricted by saturation effects. With this purpose we have analyzed the successive dissociation of n water molecules ($n = 1, \dots, 6$) at the anatase (101) surface. Figure 3 collects some representative configurations of n dissociated water molecules, $n = 1, \dots, 6$, as well as their binding energies (in eV) calculated according to the following equation:

$$E_b(n\text{diss}) = nE(\text{H}_2\text{O}, \text{gas}) + E(\text{TiO}_2) - E(n\text{H}_2\text{O}(\text{diss})/\text{TiO}_2) \quad n = 1, \dots, 6. \quad (3)$$

$E_b(n \text{ diss})$ increases steadily as the number of dissociated water molecules increases. In all cases, the distance between the oxygen atom of the hydroxyl group and the Ti5c atom oscillates around 1.8 \AA , independently of the degree of saturation of the TiO_2 surface. The comparison of Figures 1 and 3 reveals that the adsorption energies of the intact water molecules are very similar to the adsorption energies of the dissociated molecules. The successive binding energies for each new dissociated water molecule are given in Table 2. As in the case of molecular adsorption, we have calculated the VdW-corrected binding energies. Again, the effect of dispersion is to add a constant $\sim 0.2 \text{ eV}$ extra binding for each adsorbing water molecule. Let us note that the DFT binding energies show some sensitivity to the sites occupied by the dissociation fragments, varying from 0.5 up to 0.8 eV . Since the energies do not decrease by increasing the

number of dissociated molecules, it is clear that water dissociation at the surface is not a competitive process, and the surface can become easily hydroxylated under standard reaction conditions.

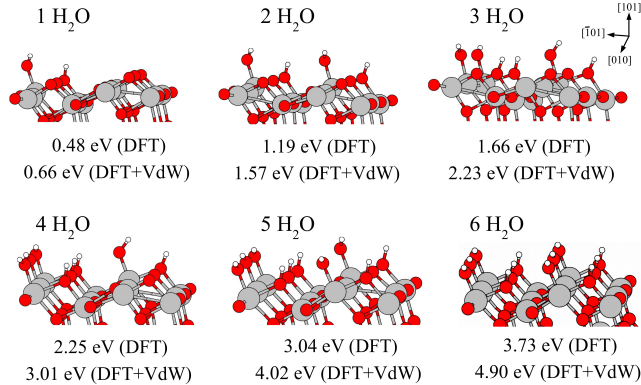


Figure 3: Equilibrium structures of n dissociated water molecules ($n = 1, \dots, 6$) as well as their binding energies (in eV). As in Figure 1, both DFT and DFT-VdW values for E_b are given.

n	1	2	3	4	5	6
$\Delta E_b(n)$ (DFT)	0.48	0.71	0.47	0.59	0.79	0.69
E_{vdw}	0.18	0.20	0.19	0.19	0.22	0.19
$\Delta E_b(n)$ (DFT+VdW)	0.66	0.91	0.66	0.78	1.01	0.88

Table 2: Successive binding energies $\Delta E_b(n)$ for dissociated water molecules on TiO₂. Energies are given in eV. As in Table 1, both DFT and DFT-VdW data are given.

Since it is evident that the anatase surface will contain sizable amounts of added OH and H species (one on top of Ti5c, the other on top of O2c atoms), it is interesting to study the mobility of these entities on the surface. In particular, one plausible reaction to take place at the anatase (101) surface covered by dissociated water molecules could be the recombination of two hydrogen atoms to form H₂ (perhaps aided by gold catalysts) followed by its desorption, leading to a situation where a higher concentration of OH radicals are adsorbed on the surface. If such process is to take place, it is first mandatory that the added hydrogen atoms should be able to diffuse from one O2c site to another. We have therefore examined the diffusion of a H atom, by analyzing two different diffusion paths between O2c sites. In the first case, the H atom attached to an O2c atom moves to another O2c atom via an intermediate O3c position (Figure 4, panel (a)). The reaction pathway can be split in two successive symmetrical steps, i.e., the H atom moves first from the O2c site to the intermediate O3c site, and then from the O3c site to the other O2c site. Only the first step is represented in panel (a) of Figure 4. In the initial state, the H atom is at a distance of 0.98 Å from the O2c atom and at 2.2 Å from the O3c atom. The

transition state occurs for the H atom approximately midway between the O2c and O3c atoms, and the height of the barrier is 0.68 eV. Then, the H atom ends up bonded to the O3c with a distance $d(\text{H-O3c}) = 0.98 \text{ \AA}$. As indicated above, this is the intermediate step, and another (symmetrical) jump from the O3c to the final O2c position is required. An alternative reaction pathway for the H diffusion between the two O2c atoms is shown in panel (b) of Figure 4. The initial state is the same as in panel (a) but the diffusion pathway is direct, without the intermediate step. In the transition state, where the H atom is placed at approximate distances of 1.0 and 1.8 \AA from the two O2c atoms, respectively, the height of the barrier is 0.61 eV. Both reaction pathways are likely to occur at moderate temperatures, with energy barriers lower than 0.7 eV, with the second one being more favorable.

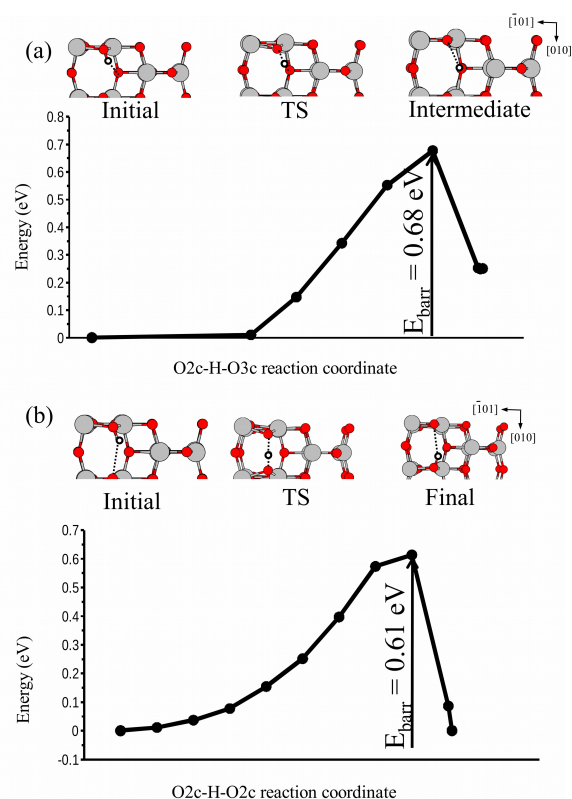


Figure 4: (a) Diffusion barrier for the motion of the H atom from an O2c to another O2c atom. In panel (a) the H atom diffuses through an intermediate step in which the H atom is on a O3c atom. The panel only shows the energies for the path between the initial state and the intermediate step. (b) Diffusion barrier for the motion of the H atom directly from an O2c to another O2c atom.

The process of hydrogen recombination can take place only if the accumula-

tion of excess OH is not thermodynamically unfavourable. For the clean anatase surface, we have analyzed this issue by studying the stability of an excess of hydroxyl groups. Figure 5 shows the results obtained for the progressive saturation of the TiO_2 surface with up to 6 hydroxyls. The cumulative binding energies $E_b(n)$, calculated with respect to the free OH radicals,

$$E_b(n) = nE(\text{OH}, \text{gas}) + E(\text{TiO}_2) - E((n\text{OH})/\text{TiO}_2) \quad n = 1, \dots, 6, \quad (4)$$

steadily increase with the number of adsorbed OH radicals. Again, we have calculated (see table 3) the successive binding energies of the individual hydroxyl radicals, and these do not differ much from an average value of 1.0 eV. This value is actually rather small; we will see in the next section that, in the presence of a gold cluster, values of around 2.0 eV are not high enough to render the process of hydrogen recombination (in a situation with initial equal concentrations of H and OH species) thermodynamically favourable. This implies that, for clean anatase, dissociating water will produce well balanced concentrations of adsorbed H and OH species.

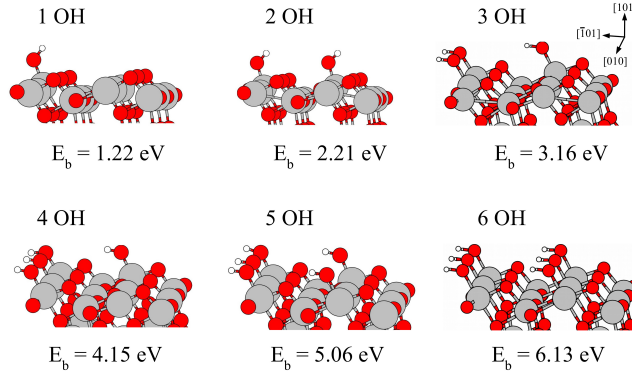


Figure 5: Equilibrium structures and total binding energies (E_b ; in eV, see eq. (4)) of n hydroxyl groups adsorbed at the anatase- $\text{TiO}_2(101)$ surface ($n = 1, \dots, 6$).

n	1	2	3	4	5	6
ΔE_b	1.22	0.98	0.95	1.00	0.91	1.07

Table 3: Successive binding energies ΔE_b for the OH hydroxyls on the TiO_2 surface. All energies are given in eV.

4. Water adsorption at an Au₄ cluster supported on anatase-TiO₂(101)

In order to investigate the possible catalytic effect of supported Au clusters on water adsorption and dissociation at the TiO₂ surface, we have first studied the stability of a single H₂O molecule adsorbed in the neighbourhood of a supported Au₄ cluster. Figure 6 shows the relaxed structures and binding energies of the most representative conformations, with the water molecule either intact (configurations a, c, e) or dissociated (configurations b, d, f). The binding energies are respectively defined

$$E_b(n) = nE(H_2O, gas) + E(Au_4/TiO_2) - E(nH_2O/Au_4/TiO_2) \quad (5)$$

and

$$E_b(n) = nE(H_2O, gas) + E(Au_4/TiO_2) - E((nH_2O(dissoc))/Au_4/TiO_2) \quad (6)$$

where, in the present case, $n = 1$. As in the case of the clean TiO₂ surface, we have analyzed the effect of adding dispersive VdW corrections to the binding energies. Again, Grimme's semiempirical correction stabilizes each conformation by a quite constant factor, now of the order of 0.25 eV. The extra 0.05 eV stabilization (with respect to the clean anatase-TiO₂ case) can be attributed to the extra VdW interaction between adsorbed water and the gold cluster). Panels a) and b) illustrate a situation where the water molecule is located close to the gold cluster, but not in direct contact with this one. The DFT binding energies are only slightly larger than those obtained for the clean anatase (101) surface (0.66 eV, as compared to 0.57 eV for the intact water molecule; and 0.57 eV, as compared to 0.48 eV for the dissociated molecule). This means that the interaction between the Au₄ cluster and the surface does not affect much the electronic structure of the TiO₂ surface. The other conformations, c) to f), illustrate situations where the water molecule is directly bonded to the supported Au₄ cluster.

Conformations c) and e) show that, whenever the adsorbed water molecule is close enough to the Au₄ cluster, one of the hydrogen atoms forms a weak bond, of strength about 0.2 eV, with the gold cluster, and this enhances the adsorption binding energy of the water molecule. The DFT binding energies are 0.92 and 0.89 eV, respectively. Conformation d) shows a different situation: water dissociation on top of a surface oxygen anion bonded to Au₄ leads to a slightly lower binding energy of the dissociated water molecule by approximately 0.1 eV compared to panel b). Finally, conformation f) illustrates another interesting

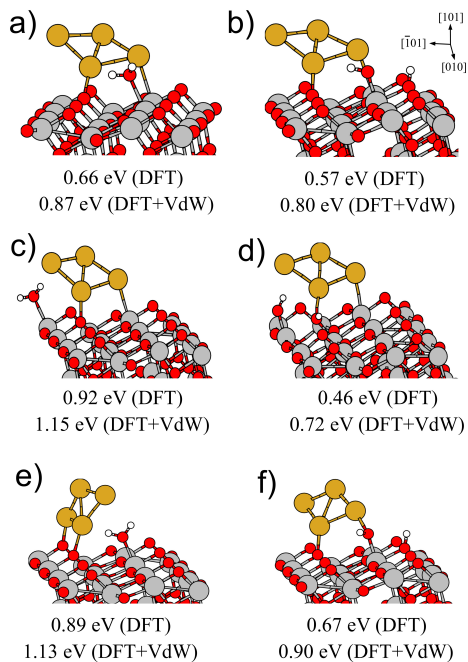


Figure 6: Equilibrium structures of a water molecule (either intact or dissociated) adsorbed near a Au_4 cluster supported on anatase- $\text{TiO}_2(101)$. Both pure DFT and VdW-corrected binding energies are given on each case.

effect: there is a favourable interaction between the gold cluster and the oxygen atom of the adsorbed OH group after water dissociation. The conclusion from the data reported in Figure 6 is that the adsorption and the dissociation of water on the surface of TiO_2 anatase is only affected by the presence of a Au_4 cluster when this is in the close neighbourhood of the water molecule.

Next we have investigated the reactivity of the TiO_2 surface towards formation of a high concentration of hydroxyl radicals, now in the presence of the adsorbed Au_4 cluster. Figure 7 gives the equilibrium conformations and the total binding energies $E_b(n)$ of up to five dissociated water molecules. $E_b(n)$ is given by equation (6). In this case, since the presence of the gold cluster causes the surface binding sites not being completely equivalent to each other, we can expect slight variations of the total binding energy for various inequivalent conformations of n adsorbed hydroxyls. Because of the large number of possible configurations, we have chosen a representative set, where for small and intermediate OH concentrations, most of the hydroxyl groups are placed away from the supported Au_4 cluster. As we did for the clean TiO_2 surface, we have calculated the successive binding energies for each additional water molecule (see Table 4). In the presence of the Au_4 cluster, there is not much influence of the coverage on the adsorption binding energy of the dissociated molecules.

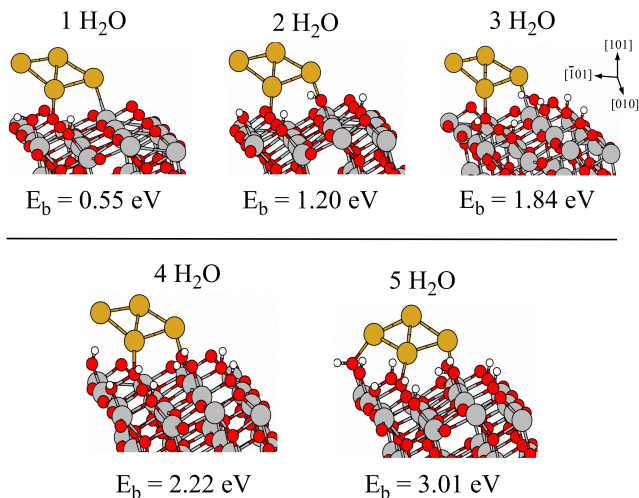


Figure 7: Equilibrium structures and binding energies of n dissociated water molecules ($n = 1-5$) on the anatase $\text{TiO}_2(101)$ surface with an adsorbed Au_4 cluster.

The decrease of the binding energy of the 4th water molecule and the slight increase for the 5th one can be explained by the way those molecules bind to the anatase surface. Dissociation of the 4th water molecule delivers a H atom adsorbed on top of a surface oxygen atom situated below the Au_4 cluster (which is slightly unfavourable, as we have seen in Figure 6d). When the 5th water molecule dissociates, the OH group formed binds to the Au_4 cluster through the oxygen atom, which results in a higher binding energy.

n	1	2	3	4	5
$\Delta E_b(n)$	0.55	0.65	0.64	0.38	0.79

Table 4: Successive binding energies, $\Delta E_b(n)$, for dissociated water molecules on a TiO_2 surface with a supported Au_4 cluster. Energies are given in eV.

n	1	2	3	4	5
$\Delta E_b(n)$	2.51	1.72	1.39	2.36	2.64

Table 5: Successive binding energies, $\Delta E_b(n)$, for the sequential adsorption of OH groups on a TiO_2 surface with a supported Au_4 cluster. Energies are given in eV.

As well as for the clean anatase surface, we have analyzed the possibility of an excess concentration of OH groups on the surface, as a result of the recombination of H atoms into H_2 molecules followed by desorption of the molecules. Figure 8 shows the equilibrium structures of up to five OH groups adsorbed on top of Ti5c surface atoms, as well as the total binding energies calculated with

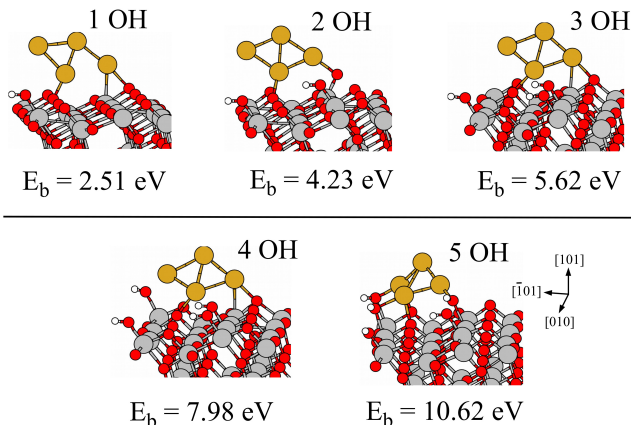


Figure 8: Equilibrium structures and total binding energies of up to five OH groups adsorbed around a supported Au_4 cluster.

respect to n free OH radicals (similar to eqn. (4)). Table V shows the successive binding energies. We observe, for the second and third OH radicals, a slightly competitive effect, reflected in a small decrease on the successive binding energies. Binding energies raise again for the 4th and 5th radicals, a result that can be explained by their special adsorption configurations, in direct contact with the supported Au_4 cluster.

Except for $n=3$, the successive OH binding energies have values between 1.7 and 2.6 eV, about double the value of the corresponding binding energies on the clean anatase surface (that is, in the absence of Au_4). Therefore, the supported Au_4 cluster greatly enhances the reactivity of TiO_2 towards the adsorption of hydroxyls, a species which strongly attracts electrons upon binding. The reason for this can be explained by comparing the electronic structure of the $\text{OH}/\text{Au}_4/\text{TiO}_2$ and the OH/TiO_2 systems. Figure 9 shows the electronic density of states (DOS) for the valence electrons in both cases, as well as the most relevant projected densities of states (PDOS). When Au_4 adsorbs on TiO_2 , the relatively high energy of the Au_4 orbitals causes some of the gold-related electronic levels (blue curve in the upper panel of Figure 9) to fall well above the top of the TiO_2 valence band. On the other hand, the $2p$ levels for the oxygen atom of adsorbed OH (red line) fall well below the top of the TiO_2 valence band. As a result, the OH adsorbate completes its 8-electron closed shell. The inset in the upper panel of the figure shows that the extra electron transferred to OH actually comes from the Au_4 orbital located within the band gap. This level, filled with two electrons in the free Au_4 cluster, is only filled with one electron in our case. We then conclude that the adsorption of OH is associated to an easy electron transfer, through the TiO_2 surface, of electrons from the deposited gold cluster to the OH group. This effect has already been reported for the adsorption of O_2 , an adsorbate which also extracts charge from the surface upon binding

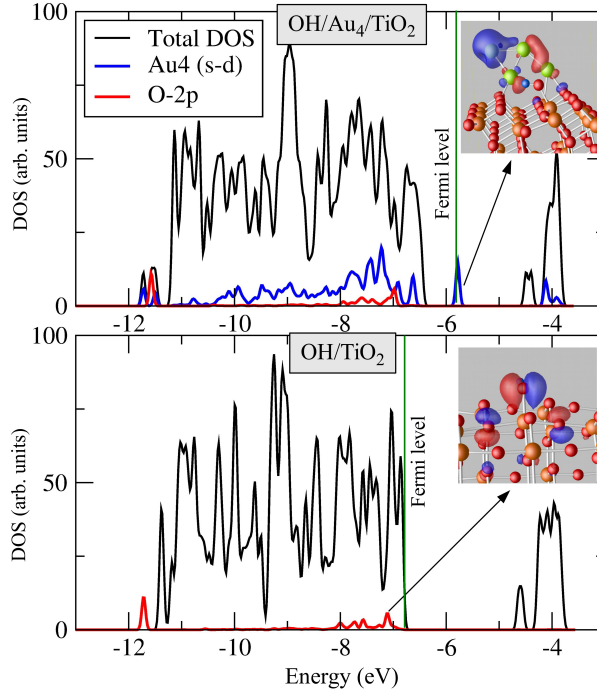


Figure 9: Top panel: Total density of electronic states (DOS) and some relevant partial densities of states (PDOS) for OH adsorbed on Au_4/TiO_2 . The vertical line indicates the position of the Fermi level. Lower panel: Analogous results for OH adsorbed on TiO_2 . In the insets, blue, red, brown and green balls correspond, respectively, to H, O, Ti and Au atoms.

[12, 13]. The lower panel shows the situation in the absence of Au_4 . Now, the adsorbed OH also extracts one electron upon binding; however, such an electron comes from the top of the TiO_2 valence band, which lies 1 eV deeper than the Au-related level of the previous case. This results in a substantial decrease in the adsorption energy of OH compared to the case with Au_4 present. The inset in the lower panel of Figure 9 shows the electron distribution for the O-2p level where the electron coming from TiO_2 is transferred.

Simulating the adsorption of OH groups allows us to calculate the energy balance of the water dissociation reaction followed by hydrogen recombination into gas phase H_2 , leaving excess OH on the surface. The corresponding reaction energy is:

$$E_{react} = E(H_2O) + E(Au_4/TiO_2) - 1/2E(H_2) - E(OH/Au_4/TiO_2) \quad (7)$$

For each OH radical adsorbed we obtain a value close to -1 eV, which means that the reaction is endothermic. This value must be compared with the corresponding value for the clean TiO₂ surface, which is about -2 eV per OH group (due to the weak OH binding). Although hydrogen recombination is unfavourable in either case, it is clear that the presence of supported gold favours excess OH concentrations. This means that, in reactions involving molecules that can be easily hydrogenated (alkenes, for example) gold may facilitate the donation of hydrogen atoms from the TiO₂ support.

5. Activation barriers for H₂O dissociation at Au₄/TiO₂

Now, we discuss the process of dissociation of H₂O at the Au₄/TiO₂ model system, by reporting the calculated energy barriers during the dissociation reaction. First, we have explored the possibility of dissociation of water directly on an isolated Au₄ cluster, without the influence of the TiO₂ surface. The reaction energy during the dissociation process is shown in Figure 10. Initially, the H₂O molecule is adsorbed on the cluster through the oxygen atom, with a moderate binding energy of 0.52 eV. At the transition state, the dissociating hydrogen atom is located fairly close to the cluster, with a bond distance to neighbouring Au atoms of around 1.7 Å. The distance between the hydroxyl group and its neighbor gold atom is also 1.7 Å. This transition state is quite unstable, with a 1.09 eV reaction barrier, and is located well above (+0.6 eV) the reference energy of the gas phase water molecule. Finally, the dissociated state (with a negative binding energy of -0.3 eV) is much less stable than the molecular one. Comparing this with the dissociation of water directly at the clean TiO₂ surface, which shows much lower barriers and a sizable binding energy for the final dissociated state, it seems unlikely that water could dissociate at Au sites not in contact with the surface.

The energy barriers for water dissociation on the TiO₂ surface, now in the neighborhood of the adsorbed Au₄ cluster, are shown in Figures 11 and 12. Four different reaction pathways have been selected. The top panel of Figure 11 shows the dissociation barrier when the water molecule is adsorbed in the neighbourhood of Au₄, but not making direct contact with the cluster. This plot is strikingly similar to the one for water dissociation on the clean anatase surface in Figure 2. In the two cases, the initial water binding energy, the barrier heights, and the stabilities of the dissociated states are nearly equal. This means again that the presence of adsorbed Au₄ does not induce severe modifications on the electronic structure of the anatase surface, which could affect the stability of transition states.

The lower panel of Figure 11 shows an alternative dissociation pathway where the water molecule initially binds to a Ti surface cation right at the perimeter of the gold cluster. As we have observed before, water binds to the Au₄ cluster through a hydrogen atom, and this enhances slightly the binding energy of the molecule to Au₄/TiO₂. Then, in order to dissociate the water molecule, that H-Au bond needs to be broken; the intermediate conformation shown in the figure illustrates the energy cost, almost 0.2 eV, of breaking such bond. The

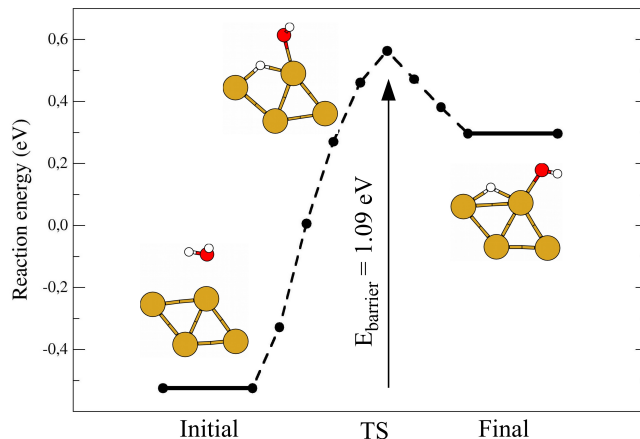


Figure 10: Barrier for the dissociation of H_2O on a free Au_4 cluster. The energy zero corresponds to gas-phase molecular water.

next inset shows the geometry of the transition state, which is very similar to the one found in the dissociation path of panel a). The hydrogen atom is again shared between the OH group and the surface oxygen anion, at a distance of 1.2 Å from either of them. The total energy barrier, measured from the initial state, is 0.69 eV. After subtracting the cost of breaking the H-Au bond, the barrier height is very similar to that in panel a).

Figure 12 shows two additional reaction pathways for water dissociation. In the upper panel, the energy profile corresponds to a slightly different initial conformation of the adsorbed Au_4 cluster. Again, a slightly larger energy barrier (of 0.74 eV) is obtained due to the cost of breaking the weak H-Au bond. In this case, the final state gets a little extra stabilization, around 0.1 eV, due to an attractive interaction between the oxygen atom of the hydroxyl group and the Au_4 cluster. Interestingly, such stabilization does not occur in the transition state. In spite of the close distance, the dissociating H_2O molecule does not bind to the gold cluster, and the binding energy at the transition state is the same as for the other cases. Finally, the lower panel of Figure 12 shows a dissociation pathway where the departing hydrogen atom binds to the oxygen surface anion bound to one of the atoms of the gold cluster. The energy barrier is again 0.7 eV. The final dissociated state is a bit less stable compared to those found for the other dissociation paths. This occurs because it is unfavourable for the hydrogen atom to form a hydroxyl group just below the Au_4 cluster, as we have already discussed in the previous section.

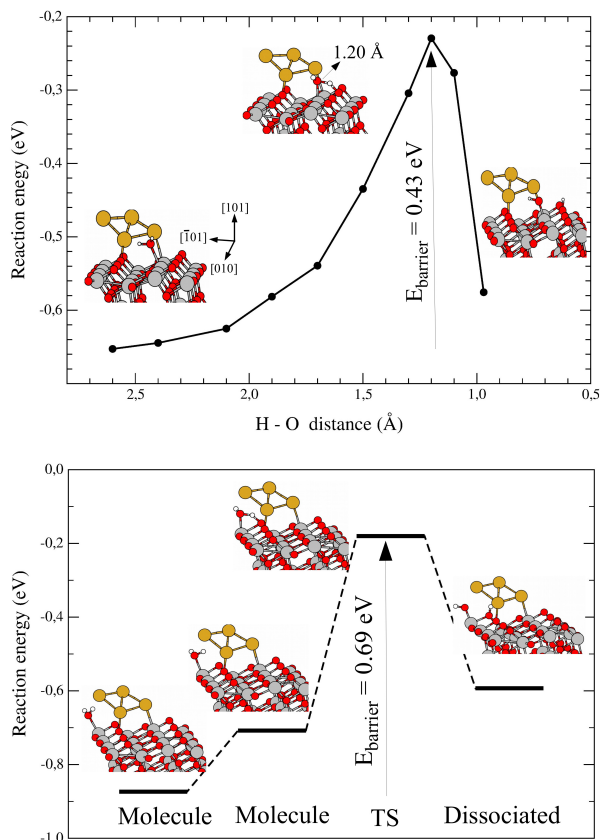


Figure 11: Barrier for dissociation of H_2O near a Au_4 cluster supported on the anatase $\text{TiO}_2(101)$ surface. The two panels correspond to two initial positions of the water molecule. The energy zero corresponds to the energy of a gas-phase water molecule.

6. Conclusions

We have studied the interaction of water with TiO_2 -supported gold nanocatalysts. In agreement with previous studies, we find that water can easily cover the bare anatase- TiO_2 (101) surface, with an adsorption energy of around 0.6 eV per molecule (0.8 eV, if VdW interactions are included). There are no competitive adsorption effects, and the binding energy per molecule is almost insensitive to the coverage. Dissociated water is only marginally (0.1 eV) less stable than molecular water; in this case competitive effects are also absent, and the binding energy per water molecule almost does not change with increasing coverage. For clean anatase- $\text{TiO}_2(101)$, we find a low activation barrier for water dissociation of only 0.41 eV; therefore, at moderate temperatures we can expect a relatively large degree of hydroxylation of the surface. As the water

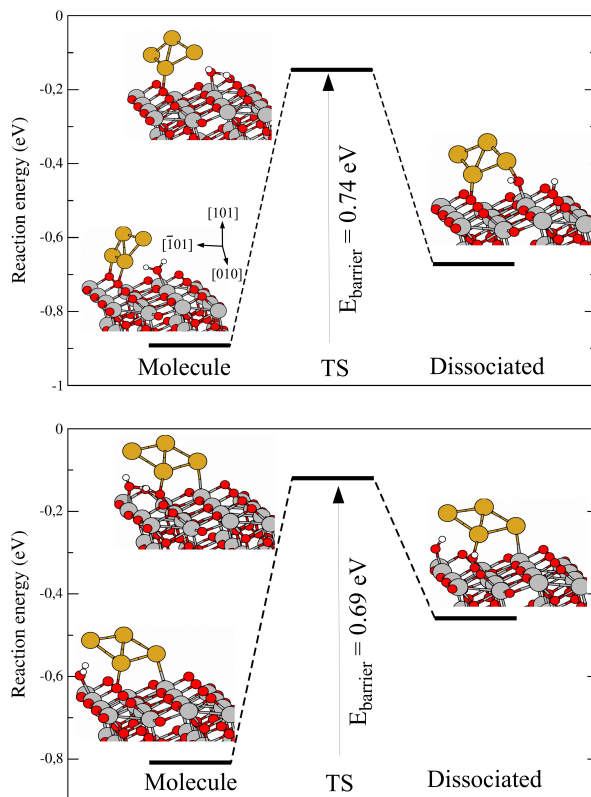


Figure 12: Barrier for dissociation of H_2O near a Au_4 cluster supported on the anatase $\text{TiO}_2(101)$ surface. The two panels correspond to different initial positions of the water molecule and the Au_4 cluster. The energy zero corresponds to the energy of a gas-phase water molecule.

coverage increases, hydrogen bonding results in even lower values for the dissociation barrier. Finally, we have calculated the diffusion barrier for hydrogen adatoms. Its moderate value (around 0.6 eV) suggests that these atoms have some mobility, and after water dissociation they may move some distance away from the neighbouring OH group. Overall, the reported energetics shows that, for any reaction which involves even minute quantities of water, a high degree of hydroxylation of the surface needs to be taken into account if one tries to correctly model the catalytic activity of any supported metal.

Next, we have placed a Au_4 cluster on the anatase surface, studying the influence of its presence on the energetics of various processes involving water adsorption and dissociation. Adsorption of molecular water is slightly stabilized on the perimeter region of the adsorbed gold cluster, due to the attractive interaction between hydrogen and gold atoms [35]. This causes a small increase

in the energy barrier for water dissociation. As a result, breaking of the water O—H bond takes place preferentially away from the cluster, with the water molecule initially bound to a titanium cation of the surface.

Finally, we have studied the stability of dissociated water in the neighbourhood of the supported cluster. There is a small stability decrease when hydroxyls are formed at O2c surface cations just below the supported Au₄ cluster. Also, due to electron transfer from the catalyst to the surface, the supported gold catalyst can favour a concentration of excess OH groups at its periphery. This means that, for reactions involving species with a tendency towards hydrogenation, surface hydrogen atoms originating from water dissociation can play an important role in the reaction. In contrast, for the bare anatase surface, any breaking of the 1:1 stoichiometry for adsorbed OH and H species is energetically unfavourable.

Acknowledgments

Work supported by the Spanish MINECO and the European Development Fund (grants MAT 2011-22781 and MAT 2014-54378-R) and by Junta de Castilla y Leon (grants VA050U14 and VA021G18). We acknowledge the support of the spanish supercomputing network (RES) by the computing time allocated at the Picasso node (University of Málaga). The authors also thankfully acknowledge the facilities provided by Centro de Proceso de Datos-Parque Científico (Universidad de Valladolid). Dr. Haydée Valdés thanks Junta de Castilla y León for a postdoctoral contract (CIP13702)

- [1] U. Diebold, Structure and properties of TiO₂ surfaces: a brief review, *Appl. Phys. A* 73 (2003) 681-687.
- [2] Z. Dohnálek, I. Lyubinetsky, R. Rousseau, Thermally-driven processes on rutile TiO₂(110)-(1x1): a direct view at the atomic scale, *Prog. Surf. Sci.* 85 (2010) 161-205.
- [3] P. Pyykko, Theoretical chemistry of gold, *Angew. Chem. Int. Ed.* 43 (2004) 4412-4456.
- [4] M. Boronat, A. Leyva-Pérez, A. Corma, Theoretical and experimental insights into the origin of the catalytic activity of subnanometric gold clusters: attempts to predict reactivity with clusters and nanoparticles of gold, *Acc. Chem. Res.* 47 (2014) 834-844.
- [5] J. A. Rodriguez, J. Evans, J. Graciani, J.-B. Park, P. Liu, J. Hrbek, J. Fdez-Sanz, High Water-Gas Shift Activity in TiO₂(110) Supported Cu and Au Nanoparticles: Role of the Oxide and Metal Particle Size, *J. Phys. Chem. C* 113 (2009) 7364-7370.
- [6] M. Daté, M. Haruta, Moisture effect on CO Oxidation over Au/TiO₂ Catalyst, *J. Catal.* 201 (2001) 221-224.

- [7] A. Bongiorno, U. Landman, Water-Enhanced Catalysis of CO Oxidation on Free and Supported Gold Nanoclusters, *Phys. Rev. Lett.* 95 (2005) 106102.
- [8] L. B. Vilhelmsen, B. Hammer, Identification of the Catalytic Site at the Interface Perimeter of Au Clusters on Rutile $\text{TiO}_2(110)$, *ACS Catal.* 4 (2014) 1626-1631.
- [9] J. Saavedra, H. A. Doan, C. J. Pursell, L. C. Grabow, B. D. Chandler, The Critical Role of Water at the Gold-Titania Interface in Catalytic CO Oxidation, *Science* 345 (2014) 1599-1602.
- [10] A. Thetford, G. J. Hutchings, S. H. Taylor, D. J. Willock, The Decomposition of H_2O_2 over the Components of Au/ TiO_2 Catalysts, *Proc. R. Soc. A* 467 (2011) 1885-1899.
- [11] X. Tong, L. Benz, S. Chretien, H. Metiu, M. T. Bowers, S. K. Buratto, Direct Visualization of Water-Induced Relocation of Au Atoms from Oxygen Vacancies on a $\text{TiO}_2(110)$ Surface, *J. Phys. Chem. C* 114 (2010) 3987-3990.
- [12] L. M. Molina, M. D. Rasmussen, B. Hammer, Adsorption of O_2 and Oxidation of CO at Au Nanoparticles Supported by $\text{TiO}_2(110)$, *J. Chem. Phys.* 120 (2004) 7673-7680.
- [13] Z. -P. Liu, X. -Q. Gong, J. Kohanoff, C. Sanchez, P. Hu, Catalytic Role of Metal Oxides in Gold-Based Catalysts: A First Principles Study of CO Oxidation on TiO_2 Supported Au, *Phys. Rev. Lett.* 91 (2003) 266102.
- [14] H. Koga, K. Tada, M. Okumura, DFT study of CO oxidation over Au/ $\text{TiO}_2(110)$: The Extent of the Reactive Perimeter Zone, *Chem. Phys. Lett.* 610 (2014) 76-81.
- [15] A. Vittadini, M. Casarin, A. Selloni, Chemistry of and on TiO_2 -Anatase Surfaces by DFT Calculations: a Partial Review, *Theor. Chem. Acc.* 117 (2007) 663-671.
- [16] C. Arrouvel, M. Digne, M. Breyse, H. Toulhoat, P. Raybaud, Effects of Morphology on Surface Hydroxyl Concentration: a DFT Comparison of Anatase- TiO_2 and γ -Alumina Catalytic Supports, *J. Catal.* 222 (2004) 152-166.
- [17] M. Posternak, A. Baldereschi, B. Delley, Dissociation of Water on Anatase TiO_2 Nanoparticles: the Role of Undercoordinated Ti Atoms at Edges, *J. Phys. Chem. C* 113 (2009) 15862-15867.
- [18] M. M. Islam, M. Calatayud, G. Pacchioni, Hydrogen Adsorption and Diffusion on the Anatase $\text{TiO}_2(101)$ Surface: A First-Principles Investigation, *J. Phys. Chem. C* 115 (2011) 6809-6814.
- [19] M. A. Saqlain, A. Hussain, M. Siddiq, A. A. Leitão, Water dissociation and CO oxidation over Au/anatase catalyst. A DFT-D2 study, *Appl. Surf. Sci.* 435 (2018) 1168-1173.

- [20] M. H. N. Assadi, D. A. H. Hanaor, The effects of copper doping on photocatalytic activity at (101) planes of anatase TiO₂: A theoretical study, *Appl. Surf. Sci.* 387 (2016) 682-689.
- [21] J. J. Mortensen, L. B. Hansen, K. W. Jacobsen, Real-Space Grid Implementation of the Projector Augmented Wave Method, *Physical Review B* 71 (2005) 035109.
- [22] J. Enkovaara, C. Rostgaard, J. J. Mortensen, J. Chen, M. Dulak, L. Ferrighi, J. Gavnholt, C. Glinsvad, V. Haikola, H. A. Hansen, *et al.* Electronic Structure Calculations with GPAW: a Real-Space Implementation of the Projector Augmented-Wave Method. *J. Phys.: Condens. Matter* 22 (2010) 253202.
- [23] J. P. Perdew, K. Burke, M. Ernzerhof, Generalized Gradient Approximation Made Simple, *Phys. Rev. Lett.* 77 (1996) 3865-3868.
- [24] M. A. L. Marques, M. J. T. Oliveira, T. Burnus, Libxc: a Library of Exchange and Correlation Functionals for Density Functional Theory, *Comput. Phys. Commun.* 183 (2012) 2272-2281.
- [25] W. Wan, X. Nie, M. J. Janik, C. Song, X. Guo, Adsorption, Dissociation, and Spillover of Hydrogen over Au/TiO₂ Catalysts: The Effects of Cluster Size and Metal-Support Interaction from DFT, *J. Phys. Chem. C* 122 (2018) 17895-17916.
- [26] R. P. Galhenage, H. Yan, S. A. Tenney, N. Park, G. Henkelman, P. Albrecht, D. R. Mullins, D. A. Chen, Understanding the Nucleation and Growth of Metals on TiO₂: Co Compared to Au, Ni, and Pt, *J. Phys. Chem. C* 117 (2013) 7191-7201.
- [27] S. Lee, C. Fan, T. Wu, S. L. Anderson, CO Oxidation on Au_n/TiO₂ Catalysts Produced by Size-Selected Cluster Deposition, *J. Am. Chem. Soc.* 126 (2004) 5682-5683.
- [28] S. Grimme, J. Antony, S. Ehrlich, H. Krieg, A consistent and accurate ab initio parametrization of density functional dispersion correction (DFT-D) for the 94 elements H-Pu, *J. Chem. Phys.* 132 (2010) 154104.
- [29] N. Kumar, P. R. C. Kent, D. J. Wesolowski, J. D. Kubicki, Modeling Water Adsorption on Rutile (110) Using van der Waals Density Functional and DFT+U Methods, *J. Phys. Chem. C*, 117 (2013) 23638-23644.
- [30] D. C. Liu, J. Nocedal, On the Limited Memory BFGS Method for Large-Scale Optimization, *Math. Program.* 45 (1989) 503-528.
- [31] A. Alavi, P. Hu, T. Deutsch, P. L. Silvestrelli, J. Hutter, CO oxidation on Pt(111): An Ab Initio Density Functional Theory Study, *Phys. Rev. Lett.* 80 (1998) 3650-3653.

- [32] P. J. D. Lindan, C. Zhang, Exothermic water dissociation on the rutile $\text{TiO}_2(110)$ surface, *Phys. Rev. B* 72 (2005) 075439.
- [33] C. E. Patrick, F. Giustino, Structure of a Water Monolayer on the Anatase $\text{TiO}_2(101)$ Surface, *Phys. Rev. Appl.* 2 (2014) 014001.
- [34] C. Dette, M. A. Pérez-Osorio, S. Mangel, F. Giustino, S. J. Jung, K. Kern, Single-Molecule Vibrational Spectroscopy of H_2O on Anatase $\text{TiO}_2(101)$, *J. Phys. Chem.* 121 (2017) 1182-1187.
- [35] L. M. Molina, J. A. Alonso, Chemical Properties of Small Au Clusters: An Analysis of the Local Site Reactivity, *J. Phys. Chem. C* 111 (2007) 6668-6677.